sustainability

MDPI

Article

Ubiquitous Occurrence of a Biogenic Sulfonate in Marine Environment

Xiaofeng Chen, Yu Han, Quanrui Chen, Huaying Lin, Shanshan Lin, Deli Wang and Kai Tang *

State Key Laboratory of Marine Environmental Science, College of Ocean and Earth Science, Xiamen University, Xiamen 361102, China; 18120757209@163.com (X.C.); yuhan1019@foxmail.com (Y.H.); wzj714354732@gmail.com (Q.C.); linhuaying99@sjtu.edu.cn (H.L.); shanshanlin@xmu.edu.cn (S.L.); deliwang@xmu.edu.cn (D.W.)

* Correspondence: tangkai@xmu.edu.cn

Abstract: The biogenic sulfonate 2,3-dihydroxypropane-1-sulfonate (DHPS) is a vital metabolic currency between phytoplankton and bacteria in marine environments. However, the occurrence and quantification of DHPS in the marine environment has not been well-characterized. In this study, we used targeted metabolomics to determine the concentration of DHPS in the Pearl River Estuary, an in situ costal mesocosm ecosystem and a hydrothermal system off Kueishantao Island. The results suggested that DHPS occurred ubiquitously in the marine environment, even in shallow-sea hydrothermal systems, at a level comparable to that of dimethylsulfoniopropionate. The concentration of DHPS was closely related to phytoplankton community composition and was especially associated with the abundance of diatoms. Epsilonproteobacteria were considered as the most likely producers of DHPS in shallow-sea hydrothermal systems. This work expands current knowledge on sulfonates and presents a new viewpoint on the sulfur cycle in hydrothermal systems.

Keywords: sulfonate; targeted metabolomics; estuary; coastal mesocosm; shallow-sea hydrothermal system

Citation: Chen, X.; Han, Y.; Chen, Q.; Lin, H.; Lin, S.; Wang, D.; Tang, K. Ubiquitous Occurrence of a Biogenic Sulfonate in Marine Environment. *Sustainability* **2022**, *14*, 1240. https://doi.org/10.3390/su14031240

Academic Editor: Jesús M. Mercado

Received: 10 December 2021
Accepted: 19 January 2022
Published: 22 January 2022

1. Introduction

Although the reservoir of sulfate in seawater greatly exceeds microbial sulfur quotas, the conversion of sulfate to organic sulfur is energetically unfavorable [1]. Sulfur that has already been reduced and incorporated into organic matter is a valuable commodity [2]. Phytoplankton-derived sulfur-containing metabolites, including sulfur-containing amino acids and their derivatives, methyl-sulfur compounds, sulfonates, and sulfate esters, could be consumed by heterotrophs on a short timescale [2,3]. Sulfonates are emerging as important chemical links between marine phytoplankton and bacteria, which, together with the well-studied sulfonium compound dimethylsulfoniopropionate (DMSP), fuel the microbial sulfur cycle in the surface ocean [2,4–6]. Among them, the C3 sulfonate 2,3-dihydroxypropane-1-sulfonate (DHPS) has been reported at millimolar cytosolic concentrations within marine diatoms and haptophytes [4], and even up to ~85 mmol/L within the sea ice diatom *Nitzschia lecointei* [7]. It has also been found as an abundant metabolite within natural plankton communities in the North Pacific and Arctic sea-ice, potentially acting as an osmolyte and/or cryoprotectant [4,7]. DHPS could be released into the dissolved matter pool, wherein it could be readily utilized by various marine heterotrophic bacteria [2,4–6,8,9]. Normally, the eutrophic coastal environment is represented as a realm containing highly active phytoplankton and bacteria, and thus likely the exhibiting DHPS cycling. Yet, few studies have been done on DHPS distribution in the coastal zones, nor have the biogeochemical characteristics influencing its abundance been well-studied.

In addition to being derived from phytoplankton, previous deep-sea research on DMSP has gradually revealed possible heterotrophic bacteria/archaea production mechanisms [10]. Additionally, DHPS has been found as the most abundant organic sulfur compound present in deep-sea hydrothermal fluids [11]. Hydrothermal *Campylobacteria* belong-

ing to Epsilonproteobacteria have been considered as the potential source of DHPS [11,12]. The relationship between DHPS and the microbial communities in these special marine environments, such as deep sea and hydrothermal environments, is still unclear. Shallow-sea hydrothermal systems, which differ substantially from their deep-sea counterparts, are generally driven by both sunlight and geothermal energy. Besides the generally predominant chemoautotrophic Epsilonproteobacteria, phytoplankton (such as cyanobacteria and diatoms) could also occur in shallow hydrothermal systems [13]. Diatoms of the genus *Thalassiosira*, members of which are high-DHPS producers [4,5], have been found in shallow-sea vents in the West Pacific [14]. Thus, we supposed that DHPS might present in shallow-sea hydrothermal systems.

To evaluate the distribution pattern of sulfur metabolites in the marine environment, we conducted an in situ monitoring of DHPS and DMSP concentrations, via targeted metabolomics, in the Pearl River Estuary and the shallow-sea hydrothermal system off Kueishantao Island, Taiwan. An in situ mesocosm experiment was performed to investigate the dynamics of DHPS and DMSP concentrations, and their relationship with the phytoplankton community. In combining with the biogeochemical characteristics, we probed into environmental factors impacting DHPS and DMSP concentrations.

2. Materials and Methods

2.1. Study Sites and Sample Collection

Samples were collected from six sites in the Pearl River Estuary, China, including three river samples (P1: 23.09° N, 113.25° E; P5: 22.94° N, 113.56° E; P7: 22.79° N, 113.63° E) and three nearshore seawater samples (A3: 22.60° N, 113.72° E; A8: 22.26° N, 113.82° E; A10: 22.14° N, 113.80° E) during 4–6 January 2017 (Figure 1). Seawater was sampled from the surface layer (~3 m below the free surface). Collections were made using 10 L Niskin bottles mounted on a rosette sampler. Biomass was collected by sequential inline filtration of seawater (0.2–0.5 L) through a nylon screen (200 μm) and a 3 μm pore-size polycarbonate filter (47 mm, Merck Millipore Ltd., Co. Cork, Ireland). After collection, the filters were immediately frozen in liquid nitrogen, then stored at −80 °C until extraction.

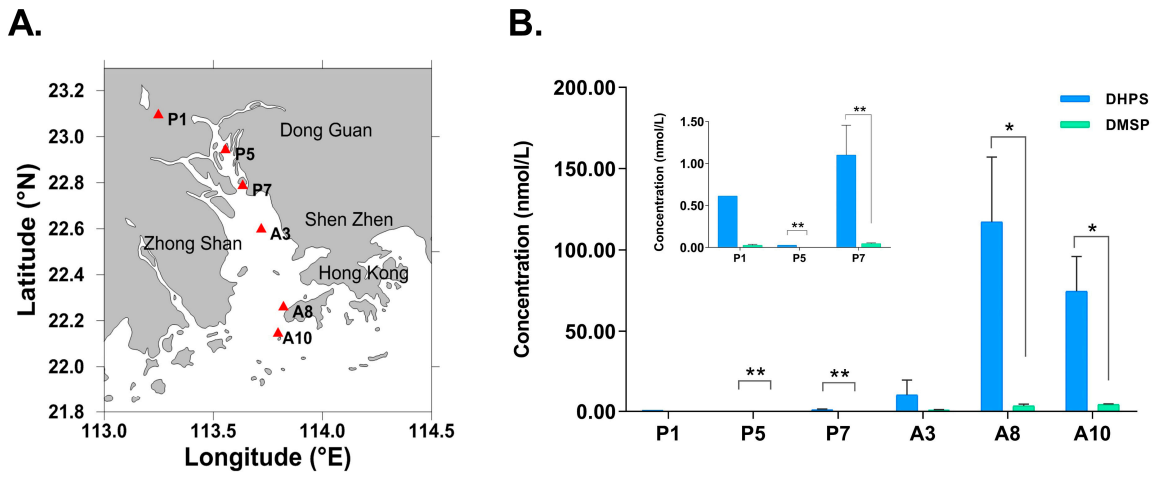

Figure 1. Map of sampling stations (**A**) and the concentrations of DHPS and DMSP in particulates (3–200 μm) (**B**) from the Pearl River Estuary. Error bars represent the standard deviation of biological triplicates (n = 3). Two-way ANOVA analysis, * $p < 0.05$, ** $p < 0.01$.

A mesocosm experiment was conducted on a floating platform at the Facility for the Study of Ocean Acidification Impacts of Xiamen University (FOANIC-XMU, 24.52° N, 118.17° E) in Wuyuan Bay, East China Sea, from 9 April to 15 May 2018. Nine cylindrical transparent thermoplastic polyurethane mesocosm bags, 3 m deep and 1.5 m wide, were set up and covered with plastic domes. Each mesocosm bag was submerged in the seawater, with 50 cm projecting above the surface. In situ seawater from Wuyuan Bay was filtered

through a water purifying system (0.01 µm pore size, MU801-4T, Media, Shenzhen, China) and pumped simultaneously into nine bags within 36 h. Four mesocosms (#2, #4, #6, and #8) were set up as control (low pCO_2, LC) and the other five mesocosms (#1, #3, #5, #7, and #9) were set up as high pCO_2 treatments (HC). To adjust seawater to the projected air conditions of ~1000 ppmv CO_2, approximately 11 L CO_2 saturation seawater were added into the five HC mesocosms. Throughout the experiment, LC and HC mesocosms were continuedly bubbled with air containing 410 and 1000 ppmv CO_2, respectively, via a CO_2 Enricher device (CE-100, Wuhan Ruihua Instrument and Equipment, China). After being prefiltered by 180 µm nylon screen, 80 L in situ seawater was used as inoculum and added into each mesocosm bag; thus, each bag contained a natural microbial community. Water was sampled from the surface layer (~0.5 m below the free surface), using a 5 L plastics Kemmerer Water Sampler. Seven of the mesocosms (HC: #1, #3, #5, #9; LC: #2, #4, #6) were chosen for further study. Mesocosm Bags 7 and 8 appear to have broken during the incubation and were not considered for the data analysis. Samples from Days 0, 11, 18, 25, and 31 were collected. After pre-filtering through 200 µm, the water samples (0.3–2 L) were filtered onto 3 µm polycarbonate filters and immediately frozen.

Sampling was performed by scuba divers on May 30 and June 2, 2019, in two different regions of the shallow-sea hydrothermal system off Kueishantao Island (24.85° N, 121.92° E), northeast Taiwan, China: the white vent (24.83° N, 121.96° E) and the yellow vent (24.834° N, 121.96° E), as well as an ambient site (24.83° N, 121.96° E) (Figure 2). The seawater was collected by plastic bags from three depths, surface (0 m below the surface), middle (5 m below the surface) and bottom layers (13.9, 8.4, and 20 m, for the white vent, the yellow vent, and ambient seawater, respectively). The seawater was pre-filtered through a nylon screen (20 µm) to remove the abundant suspended particles, then filtered in series on 3 µm-size and 0.2 µm-size polycarbonate filters (Merck Millipore Ltd., Co. Cork, Ireland). The volume of water filtered ranged from 1.4 to 2.5 L. Filters were frozen and stored at −80 °C until extraction. The filtrate was acidified with formic acid (HPLC grade), with a final concentration of approximately 0.5% (v/v) and stored at 4 °C in the dark until further extraction.

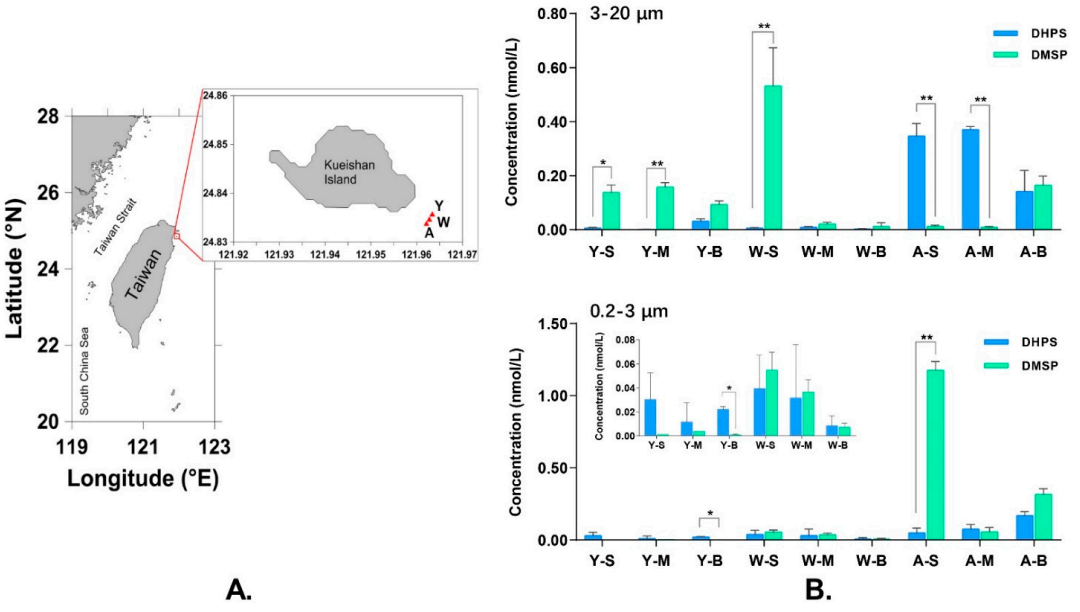

Figure 2. Map of sampling stations (**A**) and the concentrations of DHPS and DMSP in cells (3–200 µm, 0.2–3 µm) (**B**) from the shallow-sea hydrothermal systems offshore of Kueishantao Island. Y, the yellow vent; W, the white vent; A, ambient seawater; S, surface water; M, middle layer water; B, bottom water. Error bars represent the standard deviation of biological triplicates (n = 3). Two-way ANOVA analysis, * $p < 0.05$, ** $p < 0.01$.

For all sampling sites, additional water samples were taken for chlorophyll a (Chl a) analysis. The water samples (0.5–1 L) were filtered using Whatman GF/F glass fiber filters (diameter = 47 mm, pore size = 0.7 μm) and stored at −20 °C. In the Pear River Estuary, fluid samples for nutrient determination were transferred to plastic containers, and stored at 4 °C.

2.2. Determination of Biogeochemistry

Chl a was measured by a UV-VIS Spectrophotometer (DU800, Beckman, Brea, CA, USA). The temperature, pH, dissolved oxygen (DO), and salinity of seawater were measured via WTW probes (Multi 3430, Munich, Germany). Nitrite, nitrate, ammonium, and dissolved silicate were analyzed using standard colorimetric methods with a Technicon AA3 Auto-Analyzer (Bran-Luebbe, Hamburg, Germany) [15]. Total suspended material was measured via 1/10,000 electronic scale (Sartorius, Gottingen, Germany). The number of phytoplankton species of the mesocosm experiment were determined via microscopy. The environmental measurements of the Kueishantao hydrothermal systems were performed as described in [16].

2.3. Metabolite Extraction

Intracellular metabolites were extracted from the filter samples. Prior to extraction, the filters were cut into small pieces and placed at the bottom of 2 mL centrifuge tube, which contained zirconia abrasive powders. Cold (−20 °C) extraction solvent with a mixture of acetonitrile:methanol:water (40:40:20, *v*/*v*) was added to each tube and vortexed for 30 s. The sample was then crushed into a homogenate using the FastPrep system (FastPrep-24, MP Biomedicals, Irvine, CA, USA), 30 s five times, followed by incubation at −20 °C for 2 h, and centrifugation at 12,000 rpm for 15 min (4 °C). The supernatant was filtered through a 0.2 μm hydrophilic polyvinylidene fluoride (PVDF) membrane filter (13 mm, JINTENG, Tianjin, China) and transferred to an autosampler vial for the targeted metabolomics method. Known concentrations of standard analytes were added to samples before processing; these were detected and used for calculating their respective recoveries.

Extracellular metabolites were extracted from the acidified filtrate through solid phase extraction (SPE) with PPL cartridges (1 g/6 cc, Bond Elut PPL, Agilent Technologies, Folsom, CA, USA), as described in [17]. The cartridges were rinsed with two cartridge volumes of 0.1% formic acid (*v*/*v*, aqueous solution, 4 °C) and eluted with 2 mL of methanol followed by drying under clean nitrogen gas. The samples were re-dissolved in 1 mL of acetonitrile: methanol: water solution to be analyzed with the targeted metabolomics method.

2.4. Targeted Metabolomics Method

Concentrations of DHPS and DMSP were measured using an ultra high-performance liquid chromatography (UHPLC) system (1290, Agilent Technologies, Wilmington, DE, USA) with a UHPLC BEH Amide column (1.7 μm, 2.1 mm × 100 mm, Waters, Milford, MA, USA) coupled to an Agilent 6460 triple quadrupole mass spectrometer (Agilent Technologies, Wilmington, DE, USA) via an AJS electrospray ionization (AJS-ESI) interface. The methods have been described in detailed previously [8]. Multiple reaction monitoring (MRM) conditions for compounds DHPS and DMSP were optimized by infusion of authentic metabolite standards, as shown in supplementary Table S1. The parameters of operating source conditions were as described in [8]. MRM data acquisition and processing was performed by Agilent MassHunter Work Station Software (B.08.00, Agilent Technologies, Santa Clara, CA, USA). The area ratios of DHPS and DMSP were plotted relative to the targeted compounds concentration. The UHPLC separation pattern and its MS-MS fragmentation pattern were shown in the supplementary information (Figure S1).

Stock solutions of DHPS and DMSP were prepared in Milli-Q water, then combined and diluted to create gradient standard mixtures before the metabolomics analysis. Calibration curves for DHPS and DMSP were generated, with R^2 values both higher than 0.99, to determine metabolite concentrations. Considering the presence of the matrix effects [18],

the detected concentrations were further calibrated by their respective extraction efficiencies. A mixture of DHPS and DMSP was prepared as a quality control sample (QC). An in-house quality control filter considering retention time, absolute peak height, signal to noise ratio, and fragment ion ratio were used to ensure proper metabolite identification. The analytical recoveries of the QC samples were 98.4–99.8%, with all the relative standard deviations below 1.2% (n = 5). For the targeted analytes, the lower-limit of quantitation (LLOQ) was determined based on a signal-to-noise ratio of 10:1. Since the samples were analyzed in batches, we determined several LLOQs for the analytes. For samples from the Peal River Estuary, the LLOQs for DHPS and DMSP were 24.4 and 1.2 nmol/L, respectively. The LLOQs were 12.21 and 6.10 nmol/L for DHPS and DMSP, respectively, for samples from the mesocosm experiment and the Kueishantao Island hydrothermal systems. Relevant results were not used for further analysis when the concentrations were lower than the LLOQs. Targeted metabolomics data were normalized by volumes of filtrated water.

2.5. Statistical Analysis

Triplicate samples were analyzed for each site in the Pearl River Estuary and the Kueishantao hydrothermal systems, and duplicate samples for each bag of the mesocosm experiment (with day 0 and 31 exception). Data were given as mean with the standard deviation. For comparison of DHPS and DMSP concentrations, a two-way analysis of variance (ANOVA) was used, with a 95% confidence interval using GraphPad Prism version 8.0.2 (GraphPad Software, San Diego, CA, USA). Correlation between metabolite (DHPS and DMSP) concentrations and environmental parameters were examined using the non-parametric Spearman's correlation analysis, via the online SPSSAU (https://spssau.com/index.html (accessed on 21 July 2021)). GraphPad Prism version 8.0.2 was used to visualize the data.

3. Results and Discussion

3.1. Distribution of DHPS and DMSP in the Pearl River Estuary

Estuaries generally exhibit clear salinity and nutrient gradients associated with the mixture of nutrient-rich freshwater with high-salinity and low-nutrient seawater, which would significantly impact the composition, distribution, and abundance of phytoplankton [19]. The Pearl River Estuary is representative of estuaries experiencing highly eutrophication [20], which is an increasing concern. Here, we found that the concentrations of particulate DHPS exhibited a clear spatial variation, with much higher levels in offshore seawater than in the inner portion of the estuary (ranging from 0.03 to 1.50 nmol/L in river sites and from 3.27 to 150.00 nmol/L in offshore sites) (Figure 1; Table S2). DHPS and DMSP concentrations presented significantly positive correlations with pH, DO, and salinity, but a negative correlation with nutrients (Table 1). Salinity had a great effect on the distribution and composition of phytoplankton. In the presence of high levels of nutrients, high abundances of freshwater diatom species were generally found at the upstream sites, while marine diatoms and dinoflagellates primarily dominated at the zones influenced by seawater [20]. Thus, the offshore high-salinity sites contained lower phytoplankton abundances, but much higher concentrations of DHPS and DMSP (Figure 1; Table 2). It is noteworthy that although presented with a similar distribution trend, the concentration of particulate DMSP was ten-fold lower than that of DHPS (Figure 1B; Table S2). Given that diatoms, the major producers of DHPS [5], have been frequently found as the most dominant groups in the phytoplankton community of this system [20,21], the higher concentrations of DHPS than DMSP were not unexpected.

Table 1. Spearman's correlation analyses of DHPS and DMSP concentrations with environmental parameters in the Pearl River Estuary (* $p < 0.05$, ** $p < 0.01$).

Factors	DHPS	DMSP
Chl a	0.143	0.086
Temperature	−0.093	−0.309
pH	0.886 *	0.943 **
DO	0.943 **	0.886 *
Salinity	0.886 *	0.943 **
NO_2-N	−0.886 *	−0.943 **
NO_3-N	−0.943 **	−1.000 **
NH_4-N	−0.600	−0.657
DIN	−0.886 *	−0.943 **
DSi	−0.886 *	−0.943 **
TSM	−0.657	−0.600

Chl a: chlorophyll a; DO: dissolved oxygen; DIN: dissolved inorganic nitrogen; DSi: dissolved silicate; TSM: total suspended material.

Table 2. Environmental parameters in the Pearl River Estuary.

Factors	P1	P5	P7	A3	A8	A10
Chl a (μg/L)	42.99	2.61	2.05	2.19	6.12	4.98
Temperature (°C)	20.4	20.3	20.1	20.1	20.4	20.1
pH	6.98	7.11	7.37	7.74	8.24	8.30
DO (%)	25.0	44.0	62.0	81.4	103.8	101.4
Salinity (psu)	0.2	2.4	7.0	15.3	28.3	30.7
NO_2-N (μM)	35.26	14.76	13.64	7.74	1.30	0.44
NO_3-N (μM)	175.53	204.39	135.22	88.23	16.61	3.21
NH_4-N (μM)	417.38	22.68	36.55	26.44	4.63	1.85
DIN (μM)	628.17	241.82	185.41	122.41	22.53	5.50
DSi (μM)	194.45	177.98	164.87	101.93	12.72	3.12
TSM (mg/L)	42.3	44.6	21.2	41.4	24.5	28.4

Chl a: chlorophyll a; DO: dissolved oxygen; DIN: dissolved inorganic nitrogen; DSi: dissolved silicate; TSM: total suspended material.

3.2. Dynamics of DHPS and DMSP Concentrations in a Coastal Mesocosm Experiment

As a result of human activity, the atmospheric concentration of CO_2 has been increasing, leading to increased CO_2 absorption by oceans with decreasing seawater pH [22,23]. Many studies have been performed to investigate the influence of elevated pCO_2 on marine primary producers. Mesocosms are a powerful tool to maintain a natural complex community, which consider relevant aspects from "the real world" [23]. Here, we performed a field coastal mesocosm experiment to study the effects of elevated pCO_2 on the natural phytoplankton community as well as the relative concentrations of DHPS and DMSP.

A dynamic succession of the phytoplankton community occurred within these mesocosms, as previously described in [24]. Diatoms dominated the community during the early stage (occupying > 90% in terms of the total diatom + dinoflagellate species) and subsequently decreased [24], while the amounts of dinoflagellates increased after Day 16 (Figure S2A). The succession from diatoms to dinoflagellates has been frequently found in eutrophic coastal regions [25] and is attributed to their different physiological strategies in responding to environmental changes. However, the elevated CO_2 concentration impeded such succession, and the dinoflagellates did not assume dominance in the mesocosms experiencing high CO_2 concentration (Figure S2A), which was most likely due to the competitive advantages of CO_2 concentrating mechanisms in the diatoms under such conditions [24,26]. The concentration of DHPS was higher than that of DMSP during the early stage (before 18th day) of the experiment but lower than DMSP during the later stage (Figure 3 and Figure S2B; Table S2). Additionally, the concentration of DHPS was significantly positively correlated with the abundance of diatoms (Spearman, r = 0.687, $p < 0.01$), while negatively correlated with dinoflagellates abundance (r = −0.459, $p < 0.05$). The

positive correlation between DHPS and Chl a concentration (Spearman, r = 0.683, $p < 0.01$) was in line with that the greater abundance of diatoms, as these organisms would have contributed the majority of Chl a [24]. High values of particulate DMSP concentration are generally associated with dinoflagellate blooms [27–29]. Moreover, consistent with the distinction of phytoplankton community structure between two treatments, significant differences of metabolites concentrations were observed. The DHPS concentrations were significantly higher than that of DMPS in HC mesocosms, while the opposite in LC mesocosms (Figure S2B). These data indicated that the dynamics of DHPS and DMSP concentrations were most likely attributed to the change of phytoplankton community structure.

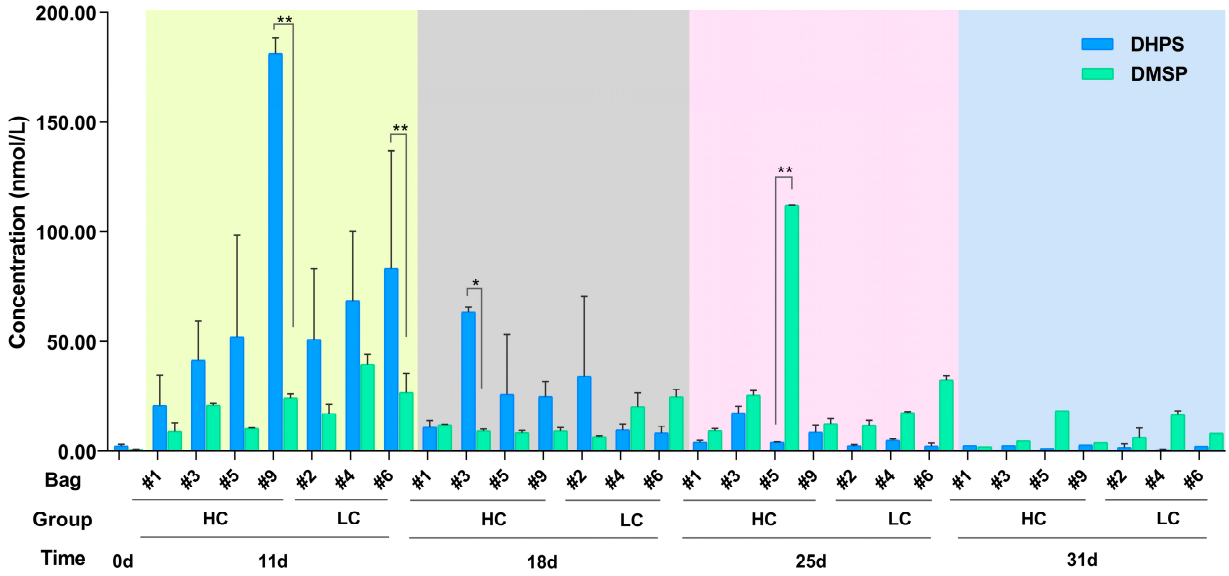

Figure 3. Particulate DHPS and DMSP concentrations during the mesocosm experiment. Error bars denote the standard deviation of biological duplicates ($n = 2$). #1–#9, indicates the order of culture bags. HC: high pCO_2 treatment groups; LC: low pCO_2 treatment groups. Two-way ANOVA analysis, * $p < 0.05$, ** $p < 0.01$.

Though the production mechanism of DHPS within phytoplankton remains unclear [4,30], our mesocosm experiment provided a basic understanding of the dynamic trend of marine sulfonate DHPS in eutrophic regions. Diatoms have been found to have a greater advantage under the combined conditions of ocean acidification and global warming, as compared to dinoflagellates [24,31]. Moreover, the abundance of diatoms, as well as the trend of the diatom to dinoflagellate ratio, would increase with increasing eutrophication and global warming, as suggested by statistical model [32]. These indicate that diatom-derived DHPS would play an increasingly important role in estuarine and coastal ecosystems, as a vital organic substrate feeding specific microorganisms [5,8], which would have ecological consequences on the microbial community and the biogeochemical cycles of carbon and sulfur.

3.3. Occurrence of DHPS and DMSP in a Shallow-Sea Hydrothermal System

Hydrothermal systems harbor spectacular communities that are primarily supported by the chemosynthesis of vent microorganisms that obtain energy from a series of redox reactions involving the reduced compounds enriched at these systems [13]. The Kueishantao hydrothermal field is a typical shallow-sea hydrothermal system, with a venting depth of <30 m, containing a mass of elemental sulfur [33,34]. Terrigenous inputs and meteoric water inputs provide labile organic matters and enable the habitation of active heterotrophic microbes as well [35,36]. Even with the presence of sunlight, such a sulfidic and highly turbid environment was not be conductive to the growth of phytoplankton, as shown by the low abundance of Chl a (0.01–0.03, 0.01–0.07, and 0.07–0.20 μg/L for the

yellow vent, the white vent, and the ambient seawater, respectively). Consistently, low nanomolar levels of biogenic organic sulfur compounds were found within phytoplankton in this ecosystem, much lower than that observed in particulates from estuary and coastal areas (Figure 2; Table S2). Interestingly, the nanomolar levels of DHPS and DMSP were observed in cells with the size of 0.2–3 μm, which are generally contained in planktonic microbial communities [37]. Epsilonproteobacteria have been observed to be the most dominant class in the Kueishantao hydrothermal system [38,39], and some members of this class can produce DHPS [12], indicating that the predominant Epsilonproteobacteria were most likely acting as the primary producers of DHPS in such ecosystems. However, no evidence has been found for the presence of a pathway involved in the production of DHPS in Epsilonproteobacteria. Future investigations are needed to address the origin of DHPS in chemoautotrophic bacteria and to assess its physiological functions in the adaption to the extreme environments.

Additionally, the dissolved DHPS extracted by SPE was detected in the seawater of the Kueishantao hydrothermal systems, with concentrations in the picomolar range, similarly to that found in deep-sea hydrothermal fluids [11]. However, the widely used solid phase Bond Elut PPL resin does not retain DHPS very well, with extraction efficiencies of less than 1% [40], which leaves their actual concentrations unclear. A challenge for future work is to develop an efficient extraction protocol for dissolved DHPS, which would be helpful for investigating ecological effects on the microbial community. The present study indicates that organic sulfur metabolites, such as DHPS, may act as a vital source for the growth of heterotrophic microorganisms inhabiting within and around the shallow-sea hydrothermal system. It would be interesting to investigate the potential ecological functions of DHPS in hydrothermal systems, for example, how DHPS impacts the hydrothermal microbial community and the carbon and sulfur cycles.

4. Conclusions

The biogenic sulfonate DHPS was widespread in estuary, coastal, and even shallow-sea hydrothermal systems. The concentration of particulate DHPS was comparable to that of DMSP, at the nanomole level. Our data suggested that the concentrations of DHPS varied in different environments and were associated with the phytoplankton community structure. The mesocosm experiment showed that diatoms were major producers of DHPS, while DMSP concentration was related to dinoflagellates amounts. With ocean acidification, diatom-derived DHPS would play an increasing important role in eutrophic coastal regions. DHPS was also detected within hydrothermal microorganisms, with Epsilonproteobacteria as the potential producers. The detection of dissolved DHPS in the shallow-sea hydrothermal system suggested its potential as organic substrates to support the growth of heterotrophic communities. This study further facilitates our understanding of the biogenic DHPS and provides a new perspective on sulfur cycle in shallow-sea hydrothermal systems.

Supplementary Materials: The following supporting information can be downloaded at: https://www.mdpi.com/article/10.3390/su14031240/s1, Table S1: MRM conditions for each metabolite; Table S2: Concentrations of DHPS and DMSP in the studied ecosystems; Figure S1: Analysis of DHPS (A) and DMSP (B) via targeted LC-MS/MS; Figure S2: Community succession of the predominate phytoplankton (A), and concentrations of DHPS and DMSP (B) during the mesoscale experiment.

Author Contributions: Conceptualization, K.T.; methodology, X.C., S.L. and D.W.; data curation, X.C.; formal analysis, X.C.; investigation, X.C., Y.H. and H.L.; visualization, X.C. and Y.H.; writing—original draft preparation, X.C., Q.C. and Y.H.; writing—review and editing, X.C., Q.C. and Y.H.; H.L., S.L., D.W. and K.T.; supervision, K.T.; project administration, K.T.; funding acquisition, D.W. and K.T. All authors have read and agreed to the published version of the manuscript.

Funding: This study was supported by the National Natural Science Foundation of China project (U1805242, 42076160, 41676070) and the International Science Partnership Program of the Chinese Academy of Sciences (121311KYSB20190029).

Institutional Review Board Statement: Not applicable.

Informed Consent Statement: Not applicable.

Data Availability Statement: Data presented in this study are contained within the article and supplementary material.

Acknowledgments: We thank Chen-Tung Arthur Chen and Bing-Jye Wang in Institute of Marine Geology and Chemistry, National Sun Yat-sen University, Wei Fan in Ocean College, Zhejiang University, and Seawatch Co., Ltd. for their assistance in collecting samples in Kueishantao hydrothermal field. We thank Nengwang Chen, Ting Lu, and Fenfang Wang in the College of Environment and Ecology, Xiamen University, for their assistance in the data measurements of environmental factors (including DO, pH, Chl a, inorganic nutrient, and other indexes) collected in Pearl River Estuary. We sincerely thank Kunshan Gao in the College of Ocean and Earth Science, Xiamen University, and his team for the help of conducting the mesocosm experiment, as well as providing the data of Chl a and phytoplankton community of mesocosms. We thank Shanghai Biotree Biomedical Biotechnology Co., Ltd., for assistance for UHPLC-MS data analysis.

Conflicts of Interest: The authors declare no conflict of interest.

References

1. Simon, J.; Kroneck, P.M. Microbial sulfite respiration. *Adv. Microb. Physiol.* **2013**, *62*, 45–117. [PubMed]
2. Moran, M.A.; Durham, B.P. Sulfur metabolites in the pelagic ocean. *Nat. Rev. Microbiol.* **2019**, *17*, 665–678. [CrossRef] [PubMed]
3. Tang, K. Chemical diversity and biochemical transformation of biogenic organic sulfur in the ocean. *Front. Mar. Sci.* **2020**, *7*, 68. [CrossRef]
4. Durham, B.P.; Boysen, A.K.; Carlson, L.T.; Groussman, R.D.; Heal, K.R.; Cain, K.R.; Morales, R.L.; Coesel, S.N.; Morris, R.M.; Ingalls, A.E.; et al. Sulfonate-based networks between eukaryotic phytoplankton and heterotrophic bacteria in the surface ocean. *Nat. Microbiol.* **2019**, *4*, 1706–1715. [CrossRef] [PubMed]
5. Durham, B.P.; Sharma, S.; Luo, H.; Smith, C.B.; Amin, S.A.; Bender, S.J.; Dearth, S.P.; Van Mooy, B.A.; Campagna, S.R.; Kujawinski, E.B.; et al. Cryptic carbon and sulfur cycling between surface ocean plankton. *Proc. Natl. Acad. Sci. USA* **2015**, *112*, 453–457. [CrossRef]
6. Durham, B.P.; Dearth, S.P.; Sharma, S.; Amin, S.A.; Smith, C.B.; Campagna, S.R.; Armbrust, E.V.; Moran, M.A. Recognition cascade and metabolite transfer in a marine bacteria-phytoplankton model system. *Environ. Microbiol.* **2017**, *19*, 3500–3513. [CrossRef]
7. Dawson, H.M.; Heal, K.R.; Boysen, A.K.; Carlson, L.T.; Ingalls, A.E.; Young, J.N.; Helmig, D.; Arrigo, K. Potential of temperature- and salinity-driven shifts in diatom compatible solute concentrations to impact biogeochemical cycling within sea ice. *Elem.-Sci. Anthrop.* **2020**, *8*, 25. [CrossRef]
8. Chen, X.; Liu, L.; Gao, X.; Dai, X.; Han, Y.; Chen, Q.; Tang, K. Metabolism of chiral sulfonate compound 2,3-dihydroxypropane-1-sulfonate (DHPS) by *Roseobacter* bacteria in marine environment. *Environ. Int.* **2021**, *157*, 106829. [CrossRef]
9. Landa, M.; Burns, A.S.; Durham, B.P.; Esson, K.; Nowinski, B.; Sharma, S.; Vorobev, A.; Nielsen, T.; Kiene, R.P.; Moran, M.A. Sulfur metabolites that facilitate oceanic phytoplankton-bacteria carbon flux. *ISME J.* **2019**, *13*, 2536–2550. [CrossRef]
10. Zhang, X.H.; Liu, J.; Liu, J.; Yang, G.; Xue, C.X.; Curson, A.R.J.; Todd, J.D. Biogenic production of DMSP and its degradation to DMS—Their roles in the global sulfur cycle. *Sci. China Life Sci.* **2019**, *62*, 1296–1319. [CrossRef]
11. Longnecker, K.; Sievert, S.M.; Sylva, S.P.; Seewald, J.S.; Kujawinski, E.B. Dissolved organic carbon compounds in deep-sea hydrothermal vent fluids from the east pacific rise at 9°50′N. *Org. Geochem.* **2018**, *125*, 41–49. [CrossRef]
12. Gotz, F.; Longnecker, K.; Kido Soule, M.C.; Becker, K.W.; McNichol, J.; Kujawinski, E.B.; Sievert, S.M. Targeted metabolomics reveals proline as a major osmolyte in the chemolithoautotroph *Sulfurimonas denitrificans*. *MicrobiologyOpen* **2018**, *7*, e00586. [CrossRef] [PubMed]
13. Tarasov, V.G.; Gebruk, A.V.; Mironov, A.N.; Moskalev, L.I. Deep-sea and shallow-water hydrothermal vent communities: Two different phenomena? *Chem. Geol.* **2005**, *224*, 5–39. [CrossRef]
14. Tarasov, V.G. Effects of shallow-water hydrothermal venting on biological communities of coastal marine ecosystems of the western Pacific. *Adv. Mar. Biol.* **2006**, *50*, 267–421.
15. Dai, M.; Lifang, W.; Guo, X.; Zhai, W.; Li, Q.; He, B.; Kao, S.-J.I. Nitrification and inorganic nitrogen distribution in a large perturbed river/estuarine system: The Pearl River Estuary, China. *Biogeosciences* **2008**, *5*, 1227–1244. [CrossRef]
16. Lin, Y.S.; Lin, H.T.; Wang, B.S.; Huang, W.J.; Lin, L.H.; Tsai, A.Y. Intense but variable autotrophic activity in a rapidly flushed shallow-water hydrothermal plume (Kueishantao islet, Taiwan). *Geobiology* **2020**, *19*, 87–101. [CrossRef]
17. Dittmar, T.; Koch, B.; Hertkorn, N.; Kattner, G. A simple and efficient method for the solid-phase extraction of dissolved organic matter (SPE-DOM) from seawater: SPE-DOM from seawater. *Limnol. Oceanogr Methods* **2008**, *6*, 230–235. [CrossRef]
18. Taylor, P.J. Matrix effects: The Achilles heel of quantitative high-performance liquid chromatography-electrospray-tandem mass spectrometry. *Clin. Biochem.* **2005**, *38*, 328–334. [CrossRef]
19. Chen, M.; Jia, H.; Su, W.; Zhang, S.; Zhao, K. Structural characteristics and associated factors influencing phytoplankton abundance and species composition in Huangmaohai bay, Pearl River Estuary. *J. Coast. Res.* **2019**, *35*, 72–81. [CrossRef]

20. Jiang, Z.-Y.; Wang, Y.-S.; Cheng, H.; Sun, C.-C.; Wu, M.-L. Variation of phytoplankton community structure from the Pearl River Estuary to South China Sea. *Ecotoxicology* **2015**, *24*, 1442–1449. [CrossRef]
21. Zong, Y.; Kemp, A.C.; Yu, F.; Lloyd, J.M.; Huang, G.; Yim, W.W.S. Diatoms from the Pearl River Estuary, China and their suitability as water salinity indicators for coastal environments. *Mar. Micropaleontol.* **2010**, *75*, 38–49. [CrossRef]
22. Orr, J.C.; Fabry, V.J.; Aumont, O.; Bopp, L.; Doney, S.C.; Feely, R.A.; Gnanadesikan, A.; Gruber, N.; Ishida, A.; Joos, F.; et al. Anthropogenic ocean acidification over the twenty-first century and its impact on calcifying organisms. *Nature* **2005**, *437*, 681–686. [CrossRef] [PubMed]
23. Riebesell, U.; Czerny, J.; von Bröckel, K.; Boxhammer, T.; Büdenbender, J.; Deckelnick, M.; Fischer, M.; Hoffmann, D.; Krug, S.A.; Lentz, U.; et al. Technical note: A mobile sea-going mesocosm system—New opportunities for ocean change research. *Biogeosciences* **2013**, *10*, 1835–1847. [CrossRef]
24. Huang, R.; Sun, J.; Yang, Y.; Jiang, X.; Wang, Z.; Song, X.; Wang, T.; Zhang, D.; Li, H.; Yi, X.; et al. Elevated pCO_2 impedes succession of phytoplankton community from diatoms to dinoflagellates along with increased abundance of viruses and bacteria. *Front. Mar. Sci.* **2021**, *8*, 642208. [CrossRef]
25. Spilling, K.; Olli, K.; Lehtoranta, J.; Kremp, A.; Tedesco, L.; Tamelander, T.; Klais, R.; Peltonen, H.; Tamminen, T. Shifting diatom—Dinoflagellate dominance during spring bloom in the Baltic Sea and its potential effects on biogeochemical cycling. *Front. Mar. Sci.* **2018**, *5*, 327. [CrossRef]
26. Giordano, M.; Beardall, J.; Raven, J.A. CO_2 concentrating mechanisms in algae: Mechanisms, environmental modulation, and evolution. *Annu. Rev. Plant Biol.* **2005**, *56*, 99–131. [CrossRef]
27. Nowinski, B.; Motard-Cote, J.; Landa, M.; Preston, C.M.; Scholin, C.A.; Birch, J.M.; Kiene, R.P.; Moran, M.A. Microdiversity and temporal dynamics of marine bacterial dimethylsulfoniopropionate genes. *Environ. Microbiol.* **2019**, *21*, 1687–1701. [CrossRef]
28. Kiene, R.P.; Nowinski, B.; Esson, K.; Preston, C.; Marin, R.; Birch, J.; Scholin, C.; Ryan, J.; Moran, M.A. Unprecedented DMSP concentrations in a massive dinoflagellate bloom in Monterey Bay, CA. *Geophys. Res. Lett.* **2019**, *46*, 12279–12288. [CrossRef]
29. Han, Y.; Jiao, N.; Zhang, Y.; Zhang, F.; He, C.; Liang, X.; Cai, R.; Shi, Q.; Tang, K. Opportunistic bacteria with reduced genomes are effective competitors for organic nitrogen compounds in coastal dinoflagellate blooms. *Microbiome* **2021**, *9*, 71. [CrossRef]
30. Denger, K.; Weiss, M.; Felux, A.K.; Schneider, A.; Mayer, C.; Spiteller, D.; Huhn, T.; Cook, A.M.; Schleheck, D. Sulphoglycolysis in *Escherichia coli* k-12 closes a gap in the biogeochemical sulphur cycle. *Nature* **2014**, *507*, 114–117. [CrossRef]
31. Chivers, W.J.; Walne, A.W.; Hays, G.C. Mismatch between marine plankton range movements and the velocity of climate change. *Nat. Commun.* **2017**, *8*, 14434. [CrossRef] [PubMed]
32. Cheung, Y.Y.; Cheung, S.; Mak, J.; Liu, K.; Xia, X.; Zhang, X.; Yung, Y.; Liu, H. Distinct interaction effects of warming and anthropogenic input on diatoms and dinoflagellates in an urbanized estuarine ecosystem. *Glob. Chang. Biol.* **2021**, *27*, 3463–3473. [CrossRef] [PubMed]
33. Chen, C.-T.A.; Zeng, Z.; Kuo, F.-W.; Yang, T.F.; Wang, B.-J.; Tu, Y.-Y. Tide-influenced acidic hydrothermal system offshore NE Taiwan. *Chem. Geol.* **2005**, *224*, 69–81. [CrossRef]
34. Zeng, Z.; Chen, C.-T.A.; Yin, X.; Zhang, X.; Wang, X.; Zhang, G.; Wang, X.; Chen, D. Origin of native sulfur ball from the Kueishantao hydrothermal field offshore northeast Taiwan: Evidence from trace and rare earth element composition. *J. Asian Earth Sci.* **2011**, *40*, 661–671. [CrossRef]
35. Price, R.E.; Giovannelli, D. Marine shallow-water hydrothermal vents: Geochemistry. In *Encyclopedia of Ocean Sciences*, 3rd ed.; Cochran, J.K., Bokuniewicz, H.J., Yager, P.L., Eds.; Academic Press: Oxford, England, 2019; Volume 4, pp. 346–352.
36. Tang, K.; Zhang, Y.; Lin, D.; Han, Y.; Chen, C.A.; Wang, D.; Lin, Y.S.; Sun, J.; Zheng, Q.; Jiao, N. Cultivation-independent and cultivation-dependent analysis of microbes in the shallow-sea hydrothermal system off Kueishantao island, Taiwan: Unmasking heterotrophic bacterial diversity and functional capacity. *Front. Microbiol.* **2018**, *9*, 279. [CrossRef] [PubMed]
37. Teeling, H.; Fuchs, B.M.; Becher, D.; Klockow, C.; Gardebrecht, A.; Bennke, C.M.; Kassabgy, M.; Huang, S.; Mann, A.J.; Waldmann, J.; et al. Substrate-controlled succession of marine bacterioplankton populations induced by a phytoplankton bloom. *Science* **2012**, *336*, 608–611. [CrossRef] [PubMed]
38. Tang, K.; Liu, K.; Jiao, N.; Zhang, Y.; Chen, C.T. Functional metagenomic investigations of microbial communities in a shallow-sea hydrothermal system. *PLoS ONE* **2013**, *8*, e72958. [CrossRef] [PubMed]
39. Zhang, Y.; Zhao, Z.; Chen, C.T.; Tang, K.; Su, J.; Jiao, N. Sulfur metabolizing microbes dominate microbial communities in andesite-hosted shallow-sea hydrothermal systems. *PLoS ONE* **2012**, *7*, e44593. [CrossRef]
40. Johnson, W.M.; Kido Soule, M.C.; Kujawinski, E.B. Extraction efficiency and quantification of dissolved metabolites in targeted marine metabolomics. *Limnol. Oceanogr. Methods* **2017**, *15*, 417–428. [CrossRef]